PERIODICA POLYTECHNICA SER. TRANSP. ENG. VOL. 35, NO. 1–2, PP. 111–123 (2007)

DEVELOPMENT OF VISUAL AND NUMERICAL METHODS BASED ON SECOND ORDER STATISTICS FOR THE ANALYSIS OF DIGITAL MEASUREMENT RECORDS

Sándor DÓRA

Department of Chassis and Lightweight Structures
Faculty of Transportation Engineering
Budapest University of Technology and Economics
H-1111 Budapest, Bertalan Lajos u. 2., Hungary
e-mail: doras@kme.bme.hu

Received: Sept. 30, 2006

Abstract

In this paper some methods developed by the author for the analysis of measurement time series containing the equally spaced sampled values of continuous-time phenomena having stable probabilistic character are introduced. The neighbourhood figure gives information about the smoothness of the record with the visualization of the second order probability density function of its nearest neighbouring values. It can be used for the fast preliminary checking of the time series. For the quantification of the visual information the neighbourhood number, a dimensionless frequency scale parameter characterizing the short-term changing rate of the record, is defined. It is suitable for the numerical rating of the smoothness of the time series and for the evaluation of the applied sampling frequency in comparison with the character of the sampled continuous function. The neighbourhood function can be used for the detection of the presence of random measurement errors. Although it gives complementary information with the autocovariance function, it is sensitive for the small deviation instead of the correlation. A method based on the extrapolation of the autocovariance function is also introduced for the numerical estimation of the magnitude of the measurement inaccuracies.

Keywords: neighbourhood figure, neighbourhood function, digitally sampled records, time series analysis.

1. Introduction

For the dynamic stressing of vehicles the applied vehicle models are usually linear dynamical systems and the excitations (e.g. road surface or profiles, water waves and atmospheric turbulence) are almost always considered as stochastic processes. The calculation procedure generally consists of the determination of the input spectral density functions from measurement records and their transformation by the frequency response function of the vehicle model. For the correct calculation of the input spectral density function it is enough that the sampling frequency applied for the measurement satisfies the Nyquist-Shannon criterion [11]. Although the preceding way of modelling gives acceptable results in practice [2], recently, a conversion to nonlinear modelling of both the excitation [3, 8] and the vehicle [9] is noticeable.

The nonlinear modelling of the excitations means the exploration and application of the deterministic natural laws characterizing the phenomena causing them. Since these laws are usually nonlinear the use of them brings on the chaotic behaviour of the system, which makes necessary the improvement of the practical methods using the tools and results of chaos theory. On the basis of the results of the initial investigations in this subject [3, 8] it can be stated that for the efficient working of the methods and tools adopted (e.g. phase portrait) a more accurate discrete representation of the phenomena taking place in continuous time is necessary, because of the application of numerical derivation and the extreme sensitivity of the chaotic systems for the boundary conditions.

Similar criteria are imposed by the usage of nonlinear vehicle models. In such cases, the spectral theorem is no more applicable for solving the excitation problem. Therefore, the calculation is based on the direct solving of the system's differential equations in the time domain by numerical integration, of which sufficient working also claims frequently sampled and smooth time series.

This study deals with some recently developed methods and analysis tools suitable for the characterization of the smoothness of the time series, for the rating of the applied sampling frequency comparing to the character of the sampled continuous function and for the estimation of the magnitude of the random measurement error. All of the procedures introduced are based on the examination of the short-term unevenness of the time series and result alternative second order statistics.

In Section 2 the neighbourhood figure, a visual tool for a preliminary fast checking of the smoothness of the record, is introduced. For the quantification of the visual information the neighbourhood number is defined and its properties are discussed in Section 3. The neighbourhood function, a sensitive tool for the presence of random measurement error, is introduced in Section 4. In the end, in Section 5 the modelling of random measurement error is examined and for the numerical estimation of its magnitude a numerical method based on the extrapolation of the autocovariance function is described.

In the following the measured continuous-time signal $\tilde{\zeta}(t)$ is considered as a realization of the stochastic process of $\tilde{\zeta}(t, \omega)$ characterizing the observed phenomenon, where ω denotes the elementary event. On the basis of physical considerations it can be assumed that the process of $\tilde{\zeta}(t, \omega)$ has a stable probabilistic mechanism and its realizations are continuous, differentiable and bounded for all ω. As a consequence of the stable probabilistic mechanism the process is assumed to be weekly stationary and ergodic for the mean value and the autocovariance function.

The measurement record is a time series containing the measured values of the continuous realization at equally spaced sampling points in the observation interval of $[0, T]$:

$$\left\{\zeta_i = \tilde{\zeta}(hi)\right\}_{i=0}^{m}; \quad T = hm. \tag{1}$$

The results introduced in the following are based on the limits [1] of the empirical statistics of this stochastic series.

2. Neighbourhood Figure

Neighbourhood figure, as its name indicates, is a graphical tool for the visualization of the relations between the nearest neighbouring values of the time series. The two dimensional set of points $\{Q_i\}_{i=0}^{m-1}$ is generated from the time series $\{\zeta_i\}_{i=0}^{m}$ by the transformation of

$$Q_i\,(\xi_i, \eta_i) = (\zeta_i, \zeta_{i+1})\,; \quad i = 0, 1, ..., m-1. \tag{2}$$

In words the coordinates of the points are equal with the adjoining values of time series. *Fig. 1* shows the neighbourhood figures of three different records, a 30 s long acceleration record measured on a point of a car body in vertical direction with sampling frequency of 300 Hz and analogue filter cut-off frequency of 30 Hz, a 200 m long dirt road profile measured with levelling with sampling interval of 10 cm and a 5 s long air flow speed measurement record of wind-tunnel turbulence digitized with sampling frequency of 2000 Hz and analogue filter cut-off frequency of 1000 Hz.

Introducing the lag number of j the definition of *Eq.* (2) can be generalized beyond the nearest neighbouring values:

$$Q_i\,(\xi_i, \eta_i) = \left(\zeta_i, \zeta_{i+j}\right)\,; \quad i = 0, 1, ..., m-j. \tag{3}$$

The multiplied lag number simulates multiplied sampling interval. The practical results can be obtained using the basic definition of *Eq.* (2), this generalized form helps only to reveal the relevant properties of the plot when $j = 1$. The generalized neighbourhood figures of the acceleration record generated with larger lag numbers can be seen in *Fig. 2*.

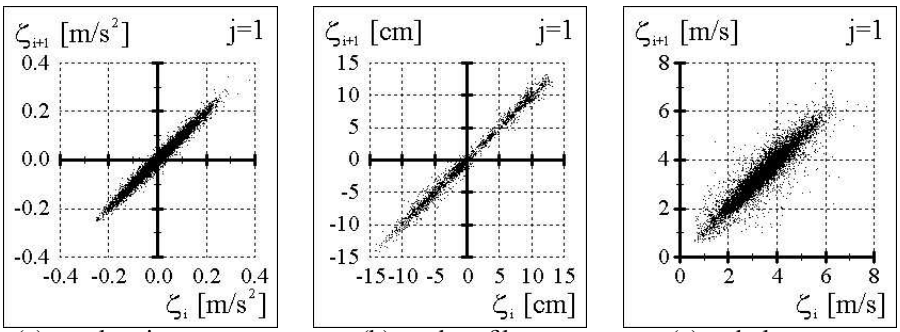

(a) acceleration (b) road profile (c) turbulence

Fig. 1. Neighbourhood figures belonging to various kinds of measurement records

The graphs in *Fig. 2* demonstrate that if the observed function $\tilde{\zeta}\,(t)$ is continuous and the sampling interval and the random measurement error are small enough, the points locate near to the $y = x$ straight line. The graphs in *Fig. 2* show that the points approach to the $y = x$ line with the decrease of the lag number, which

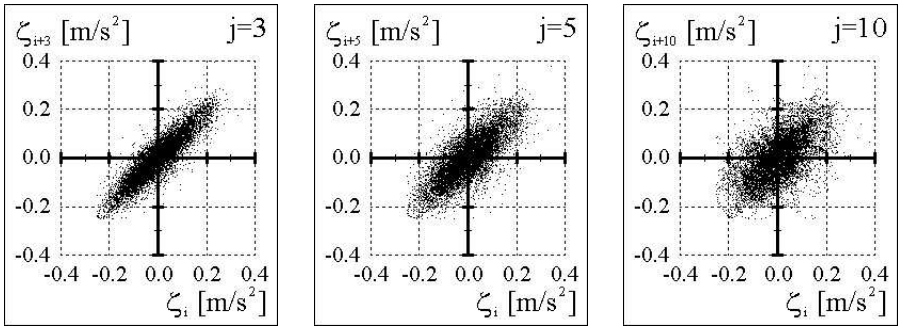

Fig. 2. Generalized neighbourhood figures generated with multiple lag numbers

is equivalent with the decrease of the sampling interval. Applying the definition of continuity it is easy to see that if there is no random measurement error, the points converge to the $y = x$ line when the sampling interval tends to zero. Summarizing, the width of the cloud of points is characteristic for the local unevenness of the time series. When the record originates from a continuous function, it depends on the relationship between the sampling frequency and the short-term unevenness character of the observed function.

Although, the defining formulas of *Eqs.* (2) and (3) are the same as that of the pseudo phase portrait generated with delay coordinates [10], the similarity is just in form and the previously diagnosed properties of the neighbourhood figures are originated in the connection with the second order marginal distributions of the time series. One of its reasons is that now only the shape of the cloud of points is in interest instead of the reconstructed trajectories.

The shape of the cloud of points sensed by the human eyes can be identified as the relative density distribution $\rho\,(x, y)$ of the points. Its exact mathematical definition is the relative number of points in unit area:

$$\rho\,(x, y) = \lim_{\substack{\Delta x \to 0 \\ \Delta y \to 0}} \frac{n\,(x, y, \Delta x, \Delta y)}{N\,\Delta y\,\Delta x}, \tag{4}$$

where $n\,(x, y, \Delta x, \Delta y)$ is the number of points in the small region of $[\Delta x, \Delta y]$ around the location of $[x, y]$ and N is the total number of points in the plot.

Applying the strong law of large numbers [1] if the vector valued random variables of $Q_i\,(\xi_i, \eta_i)$ are pairwise independent and identically distributed with the probability density function of $p_{\xi,\eta}\,(x, y)$, the relative frequency almost surely [1] tends to the probability:

$$\lim_{N \to \infty} \frac{n\,(x, y, \Delta x, \Delta y)}{N} = \int_{x-\frac{\Delta x}{2}}^{x+\frac{\Delta x}{2}} \int_{y-\frac{\Delta y}{2}}^{y+\frac{\Delta y}{2}} p_{\xi,\eta}\,(x, y)\; dy\; dx. \tag{5}$$

Performing the limiting process in *Eq.* (4) the following limit of

$$\lim_{N\to\infty} \rho\,(x, y) = p_{\xi,\eta}\,(x, y) \tag{6}$$

also exists in the sense of almost sure convergence.

If the observed process is strictly stationary in second order, the following successive equalities are valid: $p_{\xi,\eta}\,(x, y) = p^{(2)}_{\zeta}\,(x, y, j) = p^{(2)}_{\tilde{\zeta}}\,(x, y, hj)$, when $m \to \infty$ and $h = const.$ $p^{(2)}_{\zeta}\,(x, y, j)$ is the second order marginal probability density function of the stochastic series $\{\zeta_i\}$ and the first equality is based on *Eq.* (3). $p^{(2)}_{\tilde{\zeta}}\,(x, y, \tau)$ is the probability density function of the observed stochastic process $\tilde{\zeta}\,(t, \omega)$ and the second equality is the consequence of *Eq.* (1). Summarizing, the relative point density of the cloud of points in the generalized neighbourhood figures depends on the second order probability density function of the observed process, on the sampling interval and on the lag number:

$$\lim_{\substack{m\to\infty \\ h=const.}} \rho\,(x, y) = p^{(2)}_{\tilde{\zeta}}\,(x, y, hj)\,. \tag{7}$$

But this convergence is valid only in mean square [1], because the pairwise independency assumed for *Eq.* (5) is satisfied only asymptotically by the sampled values of the stochastic process $\tilde{\zeta}\,(t, \omega)$.

Eq. (7) means that all of the properties of the shape of the generalized neighbourhood figures, e.g. the symmetries discussed and illustrated in [4], are the appearance of the same properties of the second order probability density functions of the record. In the practical case when the lag number $j = 1$, the shape of the cloud (and its width as well) depends on the second order marginal probability density function $p^{(2)}_{\tilde{\zeta}}\,(x, y, h)$ of the observed process and on the sampling interval.

As a conclusion, it can be stated that the neighbourhood figure is a fast and simple tool for the visualization of the second order probability density function of the nearest neighbouring values of the time series. Thus, it is suitable for the preliminary qualitative checking of the measurement records. Its simplicity is due to the natural ability of the human eyes for the recognition of the density distribution of the cloud of points. For comparison a complex method for the numerical determination of the second order probability density function using delay coordinates can be found in [7].

3. Neighbourhood Number

For the quantitative characterization of the width of the cloud of points appearing in the neighbourhood figure, the *neighbourhood number* has been defined by the

expression

$$\delta_h = \frac{1}{\sigma_\zeta}\sqrt{\frac{1}{m}\sum_{i=0}^{m-1}(\zeta_{i+1}-\zeta_i)^2} \quad , \tag{8}$$

where σ_ζ denotes the empirical standard deviation of the discrete record and the subscript h refers to the influence of the sampling interval. Although this quantity has originally been defined as the normalized R.M.S. value of the vertical distances of the points of the neighbourhood figure from the $y = x$ straight line, it can also be originated directly from the record. Introducing the notations $\left\{\zeta_i' = \zeta_{i+1} - \zeta_i\right\}_{i=0}^{m-1}$ for the incremental time series and $\sigma_{\zeta'}$ for its empirical standard deviation, the neighbourhood number can be written in the simple form:

$$\delta_h = \frac{\sigma_{\zeta'}}{\sigma_\zeta} \quad . \tag{9}$$

If all of the realizations of the observed function $\tilde{\zeta}(t)$ are continuous and there is no random measurement error, increasing the sampling density the neighbourhood number decreases due to the diminishing of the standard deviation of the incremental time series and approaches to zero for all ω [1] when the sampling interval tends to zero [5]:

$$\lim_{\substack{h\to 0,\ m\to\infty \\ T=hm=const.}} \delta_h = 0 \quad . \tag{10}$$

If the observed function $\tilde{\zeta}(t)$ is even differentiable, another limit can also be proven in mean square sense:

$$\lim_{\substack{h\to 0,\ m\to\infty \\ T=hm\to\infty}} \frac{\delta_h}{h} = \frac{\sigma_{\dot{\tilde{\zeta}}}}{\sigma_{\tilde{\zeta}}} \quad , \tag{11}$$

where $\sigma_{\tilde{\zeta}}$ and $\sigma_{\dot{\tilde{\zeta}}}$ denote the standard deviations of the stochastic process $\tilde{\zeta}(t,\omega)$ and of its derivative $\dot{\tilde{\zeta}}(t,\omega)$.

Taking into account the definition formula of the Taylor's time scale [6] of

$$\lambda_{\tilde{\zeta}} = \frac{\sqrt{2}\sigma_{\tilde{\zeta}}}{\sqrt{-\ddot{R}_{\tilde{\zeta}}(0)}} = \sqrt{2}\frac{\sigma_{\tilde{\zeta}}}{\sigma_{\dot{\tilde{\zeta}}}} \quad , \tag{12}$$

the right hand side of *Eq.* (11) can be interpreted as a frequency scale measuring the shortterm changing rate of the continuous process $\tilde{\zeta}(t,\omega)$. Moreover, on the basis of the right hand side of *Eq.* (9) the neighbourhood number can be recognized as the same parameter of the discrete record of $\{\zeta_i\}$, a dimensionless frequency scale measuring the short-term changing rate of the time series.

Eq. (9) represents that a small value of the neighbourhood number belongs to a smooth time series and its limit value of zero in *Eq.* (10) can be considered as the case of the infinite smoothness. In case of sampled records originating from

differentiable function *Eq.* (11) clearly shows that the value of the neighbourhood number is proportional with the short-term changing rate of the observed function and with the length of the sampling interval. Using this equation without the limiting process in the opposite direction the best estimation of the Taylor's scale of the continuous process allowed by the applied sampling interval can be calculated from the neighbourhood number.

Finally, if the record contains an uncorrelated series of random variables having identical mean value and standard deviation [5] the limit of the neighbourhood number in mean square is

$$\lim_{m\to\infty} \delta_h = \sqrt{2} \quad . \tag{13}$$

The maximal possible value of 2 is obtained when the correlation coefficient between the adjoining values of the random series is -1.

4. Neighbourhood Function

Since the diminishing of the sampling interval to zero is not possible in practice, for the experimental checking of the limits of *Eqs.* (10) and (11) the *neighbourhood function*, a series of neighbourhood numbers calculated with multiple time lags, has been defined by the formula:

$$\delta_h(j) = \frac{1}{\sigma_\zeta}\sqrt{\frac{1}{m-j+1}\sum_{i=0}^{m-j}\left(\zeta_{i+j}-\zeta_i\right)^2} \quad . \tag{14}$$

If the sampling interval is small enough, the beginning trend of this function is expected to be linear according to *Eq.* (11) and its extrapolated value to zero lag number calculated with a polynomial smoothing function is expected to be near to zero in correspondence with *Eq.* (10).

Fig. 3 shows the beginning segments of the neighbourhood functions of various records. All the values as well as the extrapolated value of graph (a) are $\sqrt{2}$ inside the error margin independently the lag number as it is expected on the basis of *Eq.* (13) for uncorrelated random series. The beginning part of graph (c) is linear and the extrapolated value is practically zero in correspondence with the statements of *Eqs.* (10) and (11). It shows that the sampling was frequent enough and the measurement inaccuracies were practically negligible. The beginning segment of graph (b) is quite curved that suggests that the linear segment cannot be seen, because the sampling interval is not small enough. But with a more frequent sampling the linear part could be seen and the extrapolated value would be near to zero. In this case the sampling frequency was 2000 Hz, while the cut off frequency was 1000 Hz that seems to confirm the preceding suspicion. The beginning part of graph (d) is not curved, but gives a significantly non-zero extrapolated value. It seems that the further decrease of the sampling interval would not modify the extrapolated

value and the similarity to graph (a) suggests that the record contains a fast fluctuating component that becomes dominant at small scale and can be recognized as an additive random measurement error.

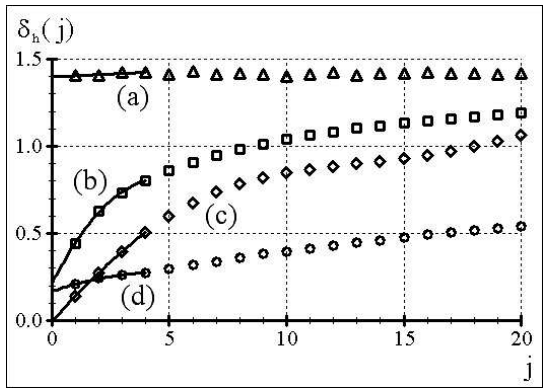

(a): series of independent Gaussian random variables, length: m = 8000
(b): turbulence, sampling: f_S = 2000 Hz, analogue filtering: f_C = 1000 Hz, length: T = 5 s
(c): acceleration record, sampling: f_S = 300 Hz, analogue filtering: f_C = 30 Hz, length: T = 30 s
(d): dirt road profile, measured with levelling, sampling interval: h = 10 cm, length: λ = 200 m

Fig. 3. Neighbourhood functions belonging to various records

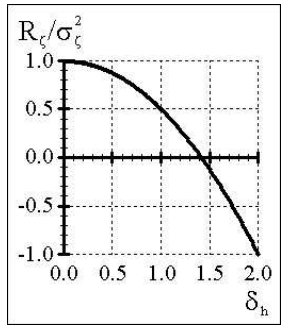

Fig. 4. Relationship between the neighbourhood and the autocovariance functions

In the following section, improved models of digital sampling taking into account measurement errors are introduced for the interpretation of the non-zero extrapolated value of the neighbourhood function. For the examination of the models, an important relationship valid in mean square sense between the neighbourhood and the autocovariance function is introduced [3]:

$$\lim_{\substack{m\to\infty \\ h=const.}} \left[\frac{\delta_h^2}{2} + \frac{R_\zeta}{\sigma_\zeta^2} \right] = 1. \tag{15}$$

The formula represents that these functions give complementary information, but the neighbourhood function (and the neighbourhood number as well) is sensitive in the domain of small deviation when the correlation is still almost perfect, while the correlation coefficient is sensitive for the weak synchronism (*Fig. 4*).

Taking into account that the beginning part of the autocorrelation function of a differentiable process can be approximated by the parabola [6] of

$$\lim_{\tau \to 0} R_{\tilde{\zeta}}(\tau) = \sigma_{\tilde{\zeta}}^2 \left[1 - \left(\frac{\tau}{\lambda_{\tilde{\zeta}}} \right)^2 \right] \tag{16}$$

and using *Eq.* (15) the linearity predicted by *Eq.* (11) can also be confirmed. This linearization is the main reason of the extreme sensitivity of the neighbourhood number and function in the domain of high correlation (*Fig. 4*).

5. Modelling and Estimation of Random Measurement Error

A simple model of the imperfect sampling suggested by the similarity between graph (a) and graph (d) in *Fig. 3* is given by the equation

$$\zeta_i = \tilde{\xi}(hi) + \eta_i \; ; \quad i = 0, 1, ..., m, \tag{17}$$

where $\tilde{\xi}(t)$ is the observed continuous function and the measurement error is taken into account as an uncorrelated random series of η_i having zero mean and identical standard deviation of σ_η added to the digitized values.

In the presence of this kind of additive discrete measurement error, on one hand, the autocovariance function of the discrete record is obtained in the form of

$$\lim_{\substack{m \to \infty \\ h = const.}} R_\zeta(j) = \begin{cases} R_{\tilde{\xi}}(0) + \sigma_\eta^2 & ; \quad j = 0 \\ R_{\tilde{\xi}}(hj) & ; \quad j \neq 0 \end{cases} , \tag{18}$$

where $R_{\tilde{\xi}}(\tau)$ is the autocovariance function of the observed process and the limit is valid in mean square. On the other hand, the neighbourhood number does not converge to zero when the sampling interval tends to zero but to the ratio of the standard deviation of the random component and the total standard deviation of the discrete record for all ω [5]:

$$\lim_{\substack{h \to 0,\ m \to \infty \\ T = hm = const.}} \delta_h = \frac{\sigma_\eta}{\sigma_\zeta} \quad . \tag{19}$$

This result accounts for the non-zero extrapolated value of the neighbourhood function.

Since the beginning segment of the neighbourhood function obtained by the substitution of *Eq.* (18) into *Eq.* (15) has an inflexion point, its polynomial smoothing

gives a biased estimation of the limit value of *Eq.* (19). Nevertheless, *Eq.* (16) is still valid, therefore, the extrapolation of the beginning segment of the autocovariance function of the time series gives acceptable result. The recommended smoothing function is a polynomial containing only even order components fitted to several beginning points except the one relating to zero lag number. The estimated value of the variance of the random measurement error is obtained by the difference between the variance of the record and the extrapolated value. Moreover, using the coefficients of the fitted curve a more accurate estimation of the Taylor's scale can also be given than that can be calculated with *Eq.* (11).

Fig. 5a illustrates the relation of *Eq.* (18), while the beginning segment of the autocovariance function of the dirt road record with the extrapolating curve, which is a sixth order parabola fitted to four points, is shown in *Fig. 5b*. The estimated variance of the random error is 0.206 cm^2.

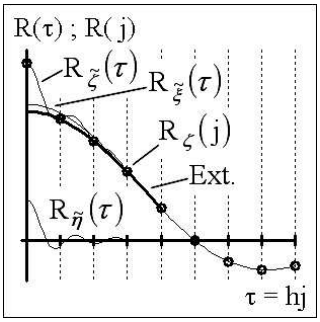

(a) Illustration

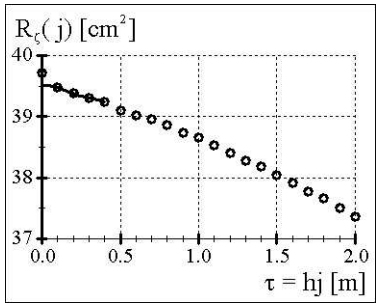

(b) Result of measurement with the extrapolating curve

Fig. 5. The autocovariance functions with the presence of discrete measurement error

Although the model of the discrete measurement error explains the non-zero extrapolated value of the neighbourhood function, it cannot be valid for all practical cases. On one hand, it can be assumed that with the decrease of the sampling interval the adjoining values of the random error become correlated. On the other hand, this model cannot represent the measurement noise occurring on the analogue side of the A/D converter.

Nevertheless, this model is valid when the time consumption of the measurement of the individual values is much less than the separation time between them. This condition is satisfied in case of relatively rarely repeated fast measurements, e.g. levelling or the determination of the rate of the flow based on the measurement of the propagation speed of disturbances in different directions.

A model suitable for the consideration of the analogue measurement noise is defined by the equation

$$\zeta_i = \tilde{\zeta}\,(hi) = \tilde{\xi}\,(hi) + \tilde{\eta}\,(hi) \quad ; \quad i = 0, 1, ..., m, \tag{20}$$

where the noise is represented by a Gaussian stochastic process of $\tilde{\eta}\,(t)$ having zero

mean and autocorrelation function of $R_{\tilde{\eta}}(\tau)$. Assuming that there is no correlation between the noise and the observed process the autocorrelation function of the record is obtained by the sum of

$$\lim_{\substack{m\to\infty \\ h=const.}} R_{\zeta}(j) = R_{\tilde{\zeta}}(hj) = R_{\tilde{\xi}}(hj) + R_{\tilde{\eta}}(hj), \tag{21}$$

where the limit is valid in mean square.

In a general case when the noise has long-term correlation the additive term $R_{\tilde{\eta}}(\tau)$ dislocates several points of the resultant autocovariance function compared to the original one. Thus, the variance of the noise cannot be sufficiently estimated by extrapolation as it is illustrated in *Fig. 6a.* However, if the correlation length of the noise is smaller than the sampling interval, which means that $\tau > h \Rightarrow R_{\tilde{\eta}}(\tau) = 0$, the summation modifies only the value of $R_{\zeta}(0)$ as it can be seen in *Fig. 6b*. Therefore, the extrapolation works well similarly to the case of the discrete error. *Fig. 6c* shows the beginning segment of the autocovariance function of the turbulence record with the extrapolating curve, which is a sixth order parabola fitted to four points. The estimated variation of the random error is 0.0307 m^2.

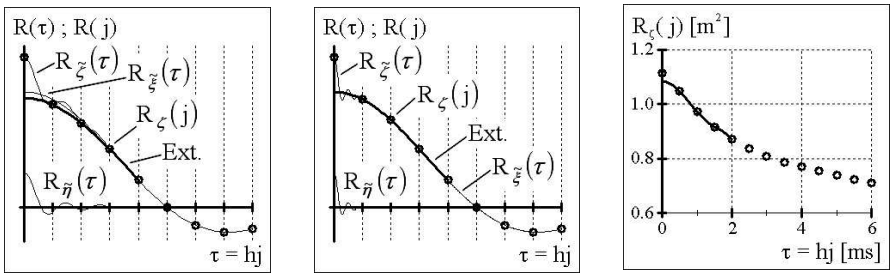

(a) Illustration of long-term correlation (b) Illustration of short-term correlation (c) Result of measurement with the extrapolating curve

Fig. 6. The autocovariance functions in the presence of fast fluctuating analogue noise

Since in practice only the autocovariance function of the discrete record is known (*Fig. 6c*), the efficiency of the estimation cannot be checked directly. Furthermore, in a general case the process of $\tilde{\eta}(t)$ can be recognized as the sum of the high frequency components of the signal at the input of the A/D converter. This part of the input signal is evaluated as measurement inaccuracy by the extrapolation method, because its fast fluctuation cannot be tracked with the applied sampling frequency. If there is any assumption or a priori knowledge about the noise sources, it can be identified with the random measurement error. However, the preceding argumentation shows that a loss of information eventuates due to sampling. The fine structure of the observed phenomena cannot be transformed to discrete form, but the variance of the lost components can be estimated.

Finally, for the checking of the estimated value of the variance of the random error a repeated calculation of the neighbourhood function is recommended accord-

ing to *Eq.* (15) after the changing of the first value of the autocovariance function to the extrapolated one.

6. Conclusions

The objective of this paper was to introduce some methods developed by the author for the analysis of digital records originating from the equally spaced sampling of continuous-time phenomena having stable probabilistic character. The neighbourhood figure and neighbourhood number are suitable for the characterization of the smoothness of the time series and for the rating of the applied sampling frequency in comparison with the changing character of the observed process. While the neighbourhood figure can be used for a fast preliminary visual checking, the neighbourhood number gives exact quantitative information.

The neighbourhood function with its extrapolating curve is an efficient tool for the detection of the presence of random measurement errors, because it is sensitive for the small dispersion of the measurement values. For the numerical estimation of the magnitude of the measurement inaccuracies an estimation procedure based on the extrapolation of the autocovariance function was also introduced.

Acknowledgement

The research reported herein has been sponsored in part by the Országos Tudományos Kutatási Alap (OTKA) under the research grant T 034537. Thanks are due to Prof. L. Laib at Gödöllő University of Agricultural Sciences for dirt road profile records and Prof. T. Lajos, head of the Department of Fluid Mechanics at Budapest University of Technology and Economics and his co-workers Dr. Zs. Szepesi and F. Paulik for records of wind-tunnel measurements. I am also indebted to my tutor Prof. József Gedeon for consultation and for reading the manuscript.

References

[1] ARNOLD, L.: *Stochastische Differentialgleichnungen*, Oldenbourg, München, 1973.

[2] BENDAT, J. S. – PIERSOL, A.G., *Random Data: Analysis and Measurement Procedures*, Wiley-Interscience, New York, 1971.

[3] DÓRA, S. – GEDEON, J., Conversion from Stochastic to Chaotic Approach in Research and Design, *Technical Soaring*, **26** (2002), pp. 124–131.

[4] DÓRA, S., Introduction of Some New Methods for Processing of Digitally Recorded Samples, Proceedigns of the microCAD 2002 International Scientific Conference, Section D: Basic Engineering Sciences, University of Miskolc, March 2002, Miskolc, pp. 25–30.

[5] DÓRA, S., Analysis of Sampled Records Using Neighbourhood Figure and Neighbourhood Function, Proceedings of the 8th Mini Conference on Vehicle System Dynamics, Identification and Anomalies, Budapest University of Technology and Economics, November 2002, Budapest, pp. 649–656.

[6] FAVRE, A. – KOVASZNAY, L. S. G.–DUMAS, R.– GAVIGLIO, J.– COANTIC, M., *La turbulence en mécanique des fluides*, Gauthier-Villars, Paris, 1976.
[7] FRASER, A. M. – SWINNEY, H. L., Independent Coordinates for Strange Attractors from Mutual Information, *Physical Review A*, **43/2** (1986), pp. 1134–1140.
[8] GEDEON, J., Converting to Chaotics and the Problem of Stationarity, *Proceedings of the 8th Mini Conference on Vehicle System Dynamics, Identification and Anomalies*, Budapest University of Technology and Economics, November 2002, Budapest, pp. 639–648.
[9] KUTI, I., Simulation of Vehicle Motions on the Basis of the Finite Element Method, *Vehicle System Dynamics*, **36/6** (2001), pp. 445–469.
[10] PACKARD, N. H. – CRUTCHFIELD, J. P. – FARMER, J. D. – SHAW, R. S., Geometry from a Time Series, *Physical Review Letters*, **45/9** (1980), pp. 712–716.
[11] SHANNON, C. E., Communication in the presence of noise, Proc. IRE, **37** (1949), pp. 10–21.